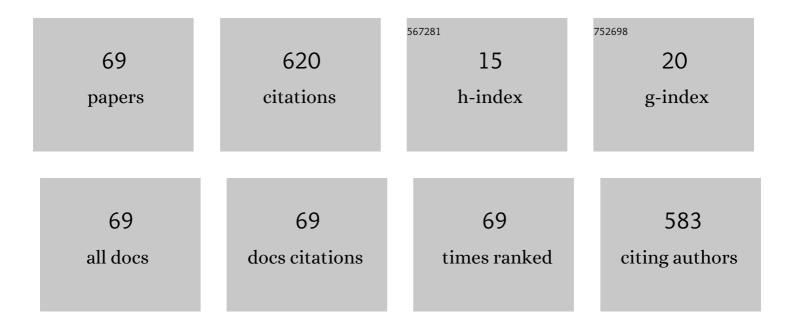
## Attila CsÃ-k

List of Publications by Year in descending order

Source: https://exaly.com/author-pdf/6307006/publications.pdf Version: 2024-02-01



Δττιι Λ CsÃi

#	Article	IF	CITATIONS
1	<p>Investigation of silver nanoparticles on titanium surface created by ion implantation technology</p> . International Journal of Nanomedicine, 2019, Volume 14, 4709-4721.	6.7	50
2	Experimental verification of thermal properties of the aerogel blanket. Case Studies in Thermal Engineering, 2021, 25, 100966.	5.7	31
3	Linear growth kinetics of nanometric silicides in Co/amorphous-Si and Co/CoSi/amorphous-Si thin films. Journal of Applied Physics, 2008, 104, .	2.5	23
4	Transition from anomalous kinetics toward Fickian diffusion for Si dissolution into amorphous Ge. Applied Physics Letters, 2008, 92, .	3.3	23
5	Metal ion-dependent tailored antibacterial activity and biological properties of polydopamine-coated titanium implants. Surface and Coatings Technology, 2019, 378, 124998.	4.8	22
6	Spontaneous near-substrate composition modulation in electrodeposited Fe–Co–Ni alloys. Electrochemistry Communications, 2009, 11, 1289-1291.	4.7	21
7	Novel amorphous Al-rich Al2O3 ultra-thin films as active photocatalysts for water treatment from some textile dyes. Ceramics International, 2020, 46, 7922-7929.	4.8	20
8	The Atomki Accelerator Centre. European Physical Journal Plus, 2021, 136, 1.	2.6	19
9	Phase growth in an amorphous Si–Cu system, as shown by a combination of SNMS, XPS, XRD and APT techniques. Acta Materialia, 2013, 61, 7173-7179.	7.9	18
10	Nanoscale investigations of shift of individual interfaces in temperature induced processes of Ni–Si system by secondary neutral mass spectrometry. Applied Physics Letters, 2010, 97, .	3.3	17
11	Calcium silicate layer on titanium fabricated by electrospray deposition. Materials Science and Engineering C, 2019, 98, 401-408.	7.3	17
12	Enhancement of Urbach's energy and non-lattice oxygen content of TiO1.7 ultra-thin films for more photocatalytic activity. Ceramics International, 2020, 46, 15236-15241.	4.8	17
13	Application of Surface Roughness Data for the Evaluation of Depth Profile Measurements of Nanoscale Multilayers. Journal of the Electrochemical Society, 2009, 156, D253.	2.9	16
14	Enhanced Physicochemical and Biological Properties of Ion-Implanted Titanium Using Electron Cyclotron Resonance Ion Sources. Materials, 2016, 9, 25.	2.9	16
15	The Effect of the PVA/Chitosan/Citric Acid Ratio on the Hydrophilicity of Electrospun Nanofiber Meshes. Polymers, 2021, 13, 3557.	4.5	15
16	Phytoliths of six woody species important in the Carpathians: characteristic phytoliths in Norway spruce needles. Vegetation History and Archaeobotany, 2019, 28, 649-662.	2.1	14
17	Preliminary studies of creation of gold nanoparticles on titanium surface towards biomedical applications. Vacuum, 2016, 126, 55-58.	3.5	12
18	Electrosprayed calcium silicate nanoparticle-coated titanium implant with improved antibacterial activity and osteogenesis. Colloids and Surfaces B: Biointerfaces, 2021, 202, 111699.	5.0	12

Attila CsÃĸ

#	Article	IF	CITATIONS
19	Nanoresolution interface studies in thin films by synchrotron xâ€ray diffraction and by using xâ€ray waveguide structure. X-Ray Spectrometry, 2009, 38, 338-342.	1.4	11
20	Production of NiSi phase by grain boundary diffusion induced solid state reaction between Ni 2 Si and Si(1 0 0) substrate. Applied Surface Science, 2014, 320, 627-633.	6.1	11
21	Coherent Light Photo-modification, Mass Transport Effect, and Surface Relief Formation in AsxS100-x Nanolayers: Absorption Edge, XPS, and Raman Spectroscopy Combined with Profilometry Study. Nanoscale Research Letters, 2017, 12, 149.	5.7	11
22	Resonance strengths in the N14 ( p,γ)O15 astrophysical key reaction measured with activation. Physical Review C, 2019, 100, .	2.9	11
23	Structural modifications induced in hydrogenated amorphous Si/Ge multilayers by heat treatments. Journal of Materials Science: Materials in Electronics, 2008, 19, 289-293.	2.2	10
24	Relationship between structural changes, hydrogen content and annealing in stacks of ultrathin Si/Ge amorphous layers. Nanoscale Research Letters, 2011, 6, 189.	5.7	10
25	In situ investigations of laser and thermally modified As2S3 nanolayers: Synchrotron radiation photoelectron spectroscopy and density functional theory calculations. Journal of Applied Physics, 2015, 118, .	2.5	9
26	Effect of heat treatments on the properties of hydrogenated amorphous silicon for PV and PVT applications. Solar Energy, 2015, 119, 225-232.	6.1	9
27	Effects of the Heat Treatment in the Properties of Fibrous Aerogel Thermal Insulation. Energies, 2019, 12, 2001.	3.1	9
28	Optimized Size and Distribution of Silver Nanoparticles on the Surface of Titanium Implant Regarding Cell Viability. Applied Sciences (Switzerland), 2020, 10, 7063.	2.5	9
29	Local surface structure and structural properties of As–Se nanolayers studied by synchrotron radiation photoelectron spectroscopy and DFT calculations. Journal of Non-Crystalline Solids, 2015, 410, 180-185.	3.1	8
30	Optical recording of surface relief on amorphous selenium. Journal of Non-Crystalline Solids, 2015, 408, 57-61.	3.1	8
31	Designing the Color of Hot-Dip Galvanized Steel Sheet Through Destructive Light Interference Using a Zn-Ti Liquid Metallic Bath. Metallurgical and Materials Transactions A: Physical Metallurgy and Materials Science, 2016, 47, 3580-3596.	2.2	8
32	Peculiar properties of preferential sputtering of PbTe, SnTe, and GeTe by Ar+ ion plasma. Materials Science in Semiconductor Processing, 2018, 88, 103-108.	4.0	8
33	Multiscale Thermal Investigations of Graphite Doped Polystyrene Thermal Insulation. Polymers, 2022, 14, 1606.	4.5	8
34	Combined Release of Antiseptic and Antibiotic Drugs from Visible Light Polymerized Biodegradable Nanocomposite Hydrogels for Periodontitis Treatment. Pharmaceutics, 2022, 14, 957.	4.5	8
35	Piezoelectric Properties of Sn2P2S6Ceramics. Ferroelectrics, Letters Section, 2006, 33, 31-38.	1.0	6
36	Oscillations and huge preferences of PbTe crystal surface sputtering under Secondary Neutral Mass Spectrometry conditions. Materials Letters, 2016, 173, 167-169.	2.6	6

Attila CsÃk

#	Article	IF	CITATIONS
37	Magnetism in structures with ferromagnetic and superconducting layers. Journal of Experimental and Theoretical Physics, 2017, 124, 114-130.	0.9	6
38	pH-dependent silicon release from phytoliths of Norway spruce (Picea abies). Journal of Paleolimnology, 2020, 63, 65-81.	1.6	6
39	The Effect of Heat Treatment of β-Tricalcium Phosphate-Containing Silica-Based Bioactive Aerogels on the Cellular Metabolism and Proliferation of MG63 Cells. Biomedicines, 2022, 10, 662.	3.2	6
40	Ti oxidation states in Zn(Ti) coating of hot-dip galvanized steels. Surface and Coatings Technology, 2017, 326, 121-125.	4.8	5
41	Laser desorption ionization time-of-flight mass spectrometry of Ge Se1 chalcogenide glasses, their thin films, and Ge:Se mixtures. Journal of Non-Crystalline Solids, 2019, 509, 65-73.	3.1	5
42	Systematic Analysis of Micro-Fiber Thermal Insulations from a Thermal Properties Point of View. Applied Sciences (Switzerland), 2021, 11, 4943.	2,5	5
43	Relaxation of the magnetic state of a ferromagnetic–superconducting layered structure. Journal of Experimental and Theoretical Physics, 2017, 125, 480-494.	0.9	4
44	Grazing-Incidence Neutron Spectrometer Detecting Neutrons and Charged Particles. Journal of Surface Investigation, 2019, 13, 478-487.	0.5	4
45	Morphological changes of poly(tetrafluoroethylene) surface due to low current density proton irradiation. Nuclear Instruments & Methods in Physics Research B, 2019, 449, 71-74.	1.4	4
46	Relative detection factor for quantification of Secondary Neutral Mass Spectrometry measurements of PbTe binary telluride. Vacuum, 2019, 163, 99-102.	3.5	4
47	Amorphisation effect in binary tellurides under low energy Ar+ ion bombardment. Materials Letters, 2019, 236, 5-8.	2.6	4
48	Reversible structural changes of in situ prepared As40Se60 nanolayers studied by XPS spectroscopy. Applied Nanoscience (Switzerland), 2019, 9, 917-924.	3.1	4
49	Possibilities of Speciation in the Central Sandy Steppe, Woody Steppe Area of the Carpathian Basin through the Example of Festuca Taxa. Forests, 2020, 11, 1325.	2.1	4
50	Near-non-preferential sputtering of multicomponent solids as an effective way for production of dense cone shape arrays on a sputtered surface. Vacuum, 2021, 186, 110058.	3.5	4
51	Evolution of the structure and hydrogen bonding configuration in annealed hydrogenated a-Si/a-Ge multilayers and layers. Applied Surface Science, 2013, 269, 12-16.	6.1	3
52	On the mechanisms of hydrogen-induced blistering in RF-sputtered amorphous Ge. CrystEngComm, 2017, 19, 1486-1494.	2.6	3
53	The behaviour of steel coated with TiB <sub>2</sub> in Sn-Ag-Cu melt. Materials Science and Technology, 2019, 35, 680-686.	1.6	3
54	Diffusion and reaction kinetics governing surface blistering in radio frequency sputtered hydrogenated a-SixGe1-x (0†â‰≇€ x†â‰≇€ 1) thin films. Thin Solid Films, 2019, 679, 58-63.	1.8	3

Attila CsÃk

#	Article	IF	CITATIONS
55	Morphology of PbTe Crystal Surface Sputtered by Argon Plasma under Secondary Neutral Mass Spectrometry Conditions. Physics and Chemistry of Solid State, 2016, 17, 336-341.	0.8	3
56	Formation of the Sputtered Phase of PbTe Crystals by Ar+ Plasma and Re-deposition of the Sputtered Species at Secondary Neutral Mass Spectrometry Conditions. Physics and Chemistry of Solid State, 2017, 18, 21-28.	0.8	3
57	Investigation of the Performance of Thermally Generated Au/Ag Nanoislands for SERS and LSPR Applications. Procedia Engineering, 2016, 168, 1152-1155.	1.2	2
58	Dissolution of thin TaV2 during annealing of Ta/TaV2/V tri-layer below the order-disorder temperature. Applied Surface Science, 2019, 466, 381-384.	6.1	2
59	Polarized Neutron Reflectrometer with the Recording of Neutrons and Gamma Quanta. Journal of Surface Investigation, 2021, 15, 549-562.	0.5	2
60	Transformations of micron-sized PbTe surface structures induced by low energy ions. Journal of Alloys and Compounds, 2021, 883, 160978.	5.5	2
61	Electrodeposition of Tin Selenide from Oxalate-Based Aqueous Solution. Journal of the Electrochemical Society, 2020, 167, 162502.	2.9	2
62	Functionalization of Amorphous Chalcogenide and Titanium Oxide Layers by Gold Nanoparticles. Advanced Materials Research, 0, 747, 289-292.	0.3	1
63	Direct surface patterning of amorphous chalcogenide layers with high- energy H+ and He+ ion beams. Journal of Materials Science: Materials in Electronics, 2019, 30, 15331-15338.	2.2	1
64	Implantation of multiply charged silicon ions into bioinert zirconia. Vacuum, 2019, 164, 15-17.	3.5	1
65	Analyzing of lead, tin and germanium tellurides by means of secondary neutral mass spectrometry: Features, problems and possibilities. Materials Today: Proceedings, 2021, 35, 513-517.	1.8	1
66	Darkening of amorphous SixGe1-x thin films by means of non-affine thermal strain. Journal of Non-Crystalline Solids, 2020, 545, 120242.	3.1	0
67	Reversible laser-assisted structural modification of the surface of As-rich nanolayers for active photonics media. Applied Surface Science, 2020, 518, 146240.	6.1	0
68	MagyarorszÃjgon forgalmazott ZrO2 (Y2O3) kerÃjmiÃjk fontosabb tulajdonsÃjgainak összehasonlÃŧó vizsgÃjlata. Fogorvosi Szemle, 2019, 112, 110-116.	0.0	0
69	Sputtering rate of lead, tin and germanium tellurides with low energy argon ions. Computational Problems of Electrical Engineering, 2021, 11, 36-41.	0.2	0